PNAS RESEARCH ARTICLE | CELL BIOLOGY

LRBA is essential for urinary concentration and body water homeostasis

Yu Hara[a], Fumiaki Ando[a,1,2], Daisuke Oikawa[b], Koichiro Ichimura[c], Hideki Yanagawa[a], Yuriko Sakamaki[d], Azuma Nanamatsu[a], Tamami Fujiki[a], Shuichi Mori[e], Soichiro Suzuki[a], Naofumi Yui[a], Shintaro Mandai[a], Koichiro Susa[a], Takayasu Mori[a], Eisei Sohara[a], Tatemitsu Rai[a], Mikiko Takahashi[f], Sei Sasaki[g,h], Hiroyuki Kagechika[e], Fuminori Tokunaga[b], and Shinichi Uchida[a,1,2]

Edited by Peter Agre, Johns Hopkins Bloomberg School of Public Health, Baltimore, MD; received February 6, 2022; accepted June 6, 2022

Protein kinase A (PKA) directly phosphorylates aquaporin-2 (AQP2) water channels in renal collecting ducts to reabsorb water from urine for the maintenance of systemic water homeostasis. More than 50 functionally distinct PKA-anchoring proteins (AKAPs) respectively create compartmentalized PKA signaling to determine the substrate specificity of PKA. Identification of an AKAP responsible for AQP2 phosphorylation is an essential step toward elucidating the molecular mechanisms of urinary concentration. PKA activation by several compounds is a novel screening strategy to uncover PKA substrates whose phosphorylation levels were nearly perfectly correlated with that of AQP2. The leading candidate in this assay proved to be an AKAP termed lipopolysaccharide-responsive and beige-like anchor protein (LRBA). We found that LRBA colocalized with AQP2 in vivo, and *Lrba* knockout mice displayed a polyuric phenotype with severely impaired AQP2 phosphorylation. Most of the PKA substrates other than AQP2 were adequately phosphorylated by PKA in the absence of LRBA, demonstrating that LRBA-anchored PKA preferentially phosphorylated AQP2 in renal collecting ducts. Furthermore, the LRBA–PKA interaction, rather than other AKAP–PKA interactions, was robustly dissociated by PKA activation. AKAP–PKA interaction inhibitors have attracted attention for their ability to directly phosphorylate AQP2. Therefore, the LRBA–PKA interaction is a promising drug target for the development of anti-aquaretics.

LRBA | AQP2 | PKA | AKAP | urinary concentration

Significance

Water transport via aquaporin-2 (AQP2) water channels is a critical determinant of urine volume. Antidiuretic hormone vasopressin activates renal protein kinase A (PKA) and then directly phosphorylates AQP2, which promotes AQP2 translocation from intracellular vesicles to the plasma membrane. We found that lipopolysaccharide-responsive beige-like anchor protein (LRBA) was a PKA-anchoring protein essential for AQP2 phosphorylation. LRBA and AQP2 were colocalized on the same intracellular vesicles, and *Lrba* knockout severely impaired PKA-induced AQP2 phosphorylation, causing high urine output. LRBA contributes to vesicular trafficking and receptor recycling of a checkpoint immune molecule, CTLA-4, in regulatory T cells. LRBA may increase plasma membrane expression levels of constitutively recycled proteins. We furthermore identified that the LRBA–PKA interaction is a drug target for polyuria.

Aquaporin-2 (AQP2) water channels in the kidneys play an essential role in the maintenance of body-water homeostasis. Under a dehydrated state, the antidiuretic hormone vasopressin is released from the posterior pituitary and binds to vasopressin type 2 receptor (V2R) in renal collecting ducts, leading to the activation of AQP2 to reabsorb water from urine for the prevention of further water loss. A lack of water homeostasis causes abnormalities in urine volume, resulting in a water–electrolyte imbalance. Loss-of-function mutations in the V2R cause X-linked congenital nephrogenic diabetes insipidus (NDI). Due to renal unresponsiveness to vasopressin, patients' urine volume reaches as much as 10 to 20 L/d (1). These patients are at a high risk of mental retardation resulting from recurrent severe hypernatremic dehydration, with a worsening prognosis (2, 3). Therefore, identifying novel mechanisms in the regulation of AQP2 is expected to be crucial in the development of anti-aquaretic drugs for the treatment of intractable polyuria.

In the canonical V2R-dependent signaling pathway, vasopressin increases intracellular cyclic adenosine monophosphate (cAMP) levels, leading to the activation of cAMP-dependent protein kinase, PKA (4). PKA is a tetramer composed of two regulatory (PKA R) and two catalytic (PKA C) subunits, and the PKA R subunits comprise four isoforms: RIα, RIβ, RIIα, and RIIβ. The second-messenger cAMP binds to PKA R subunits to change their conformation (5). Subsequently, PKA C subunits phosphorylate a wide range of cellular targets that contain the PKA recognition motif, RRXS/T. In renal collecting ducts, AQP2-S256 ($RRQS^{256}$) is directly phosphorylated by PKA (6). S256 is considered a master regulator of AQP2 activity because the phospho-mimicking mutant AQP2-S256D is predominantly localized at the apical plasma membrane to increase transcellular water transport through AQP2, whereas AQP2-S256A, which mimics nonphosphorylated AQP2, is retained in intracellular vesicles (7, 8). Phosphorylation at S256 is also important for the phosphorylation of other AQP2 C-terminal serines, such as S269 (6). pAQP2-S269 reflects AQP2 activity and correlates well with apical surface localization of AQP2 (9). Although PKA has been proven to be involved in AQP2 phosphorylation (10), critical mediators in this phosphorylation process have remained unknown.

The intracellular localization of PKA is tightly regulated by its scaffold proteins, A-kinase anchoring proteins (AKAPs). Currently, 43 AKAP genes and more than 70

The authors declare no competing interest.

This article is a PNAS Direct Submission.

[1]F.A. and S.U. contributed equally to this work.

[2]To whom correspondence may be addressed. Email: fandkidc@tmd.ac.jp or suchida.kid@tmd.ac.jp.

This article contains supporting information online at http://www.pnas.org/lookup/suppl/doi:10.1073/pnas.2202125119/-/DCSupplemental.

Published July 21, 2022.

distinct AKAP proteins have been identified (11). These AKAPs serve as subcellular "address tags" in each cell that sequester PKA to specific compartments, facilitating spatially restricted cAMP/PKA signaling to ensure substrate specificity of PKA (12). It has been reported that the AKAP220–PKA and AKAP18δ–PKA complexes are colocalized with AQP2 and participate in PKA-induced AQP2 phosphorylation (13, 14); however, there are currently no available AKAP-knockout mice that exhibit an obvious phenotype of polyuria caused by impaired AQP2 phosphorylation (15, 16). In this article, we show that lipopolysaccharide-responsive and beige-like anchor protein (LRBA) (17) is a crucial AKAP for vasopressin/AQP2 signaling. The interaction of LRBA with PKA was previously demonstrated in a B cell lymphoma cell line and in primary human B cells (18); however, its physiological relevance, especially in the renal collecting ducts, has not yet been established.

LRBA directly binds to cytotoxic T lymphocyte antigen-4 (CTLA-4) and regulates the intracellular trafficking of CTLA-4–containing vesicles in T cells (19). CTLA-4 is continually internalized via endocytosis; LRBA–CTLA-4 interaction rescues CTLA-4 from lysosomal degradation, allowing the recycling of CTLA-4 back to the cell surface, where it counteracts the activation of the immune system (20). Considering LRBA is ubiquitously expressed, it is strongly anticipated that LRBA also regulates other constitutively recycled proteins, such as AQP2. Here, we show that LRBA regulates urine-concentrating ability via mediating AQP2 phosphorylation.

Results

Correlation Between AQP2 and LRBA Phosphorylation. To identify novel critical regulators of renal water retention, we first examined the potency of a PKA activator, FMP-API-1/27, and several flavonoids on AQP2 phosphorylation at S269. Flavonoids (namely, luteolin, quercetin, naringenin, epicatechin, pelargonidin, and genistein) have been reported to enhance cAMP/PKA pathway activity by the inhibition of phosphodiesterases (21–24). Each compound had a different strength to phosphorylate AQP2-S269 in a mouse cortical-collecting-duct principal cell line (mpkCCD$_{cl4}$) (Fig. 1*A*), which exhibits the endogenous expression of AQP2 (25, 26). The V2R agonist [deamino-Cys1, d-Arg8]-vasopressin (dDAVP), was used as a positive control for PKA activation.

Furthermore, comprehensive phosphorylation statuses of PKA substrates were measured by Western blot analysis using a phospho-PKA (pPKA) substrate antibody, which recognizes phosphoproteins containing the sequence RRXpS/T (Fig. 1*A*). Notably, densitometric analysis revealed that among the multiple bands of pPKA substrates, two pPKA substrates (indicated by black arrow and red arrowhead in Fig. 1*A*) exhibited strong positive correlations with AQP2-S269 (pAQP2-S269) in their phosphorylation characteristics induced by FMP-API-1/27 and several flavonoids (Fig. 1*B* and *C*). Contrastingly, other pPKA substrates (indicated by asterisks in Fig. 1*A*) were not correlated with pAQP2-S269. These results raised the possibility that the two PKA substrates indicated by arrowheads in Fig. 1*A* were candidate mediators involved in AQP2 phosphorylation.

Immunoprecipitation with pPKA-substrate antibody followed by mass spectrometry analysis revealed that both PKA substrates (indicated by black arrow and red arrowhead in Fig. 1A) were LRBA (Fig. 1*D* and *E*). In line with this finding, we confirmed that mouse LRBA contained three distinct RRXS motifs (*SI Appendix*, Fig. S1). We then performed posttranslational modification (PTM) analysis of overexpressed LRBA using mass spectrometry to clarify the phosphorylation sites of LRBA. Both HA-V2R and Myc-LRBA were overexpressed in HEK293T cells, and then dDAVP was administered to the cells. PTM analysis revealed that RRDS^{1607} and RRIS^{2189} were phosphorylated by dDAVP (Fig. 1*F* and *SI Appendix*, Fig. S2*A* and *B*), suggesting that these two sites were also phosphorylated by FMP-API-1/27 and flavonoids in mpkCCD cells. Encouraged by these findings, we generated tools to evaluate phosphorylation and localization of LRBA in vitro and in vivo (i.e., an antibody against recombinant LRBA and *Lrba* knockout mice) (Fig. 1*G–I*, and *SI Appendix*, Fig. S3). LRBA antibody effectively pulled down endogenous LRBA (Fig. 2*A–D*). As implicated in Fig. 1*A*, phosphorylated LRBA (pLRBA) was decreased by pelargonidin and increased by dDAVP in the mpkCCD cells. Similarly, intraperitoneal administration of dDAVP increased pLRBA in mouse kidneys, whereas suppression of endogenous vasopressin secretion by water load decreased pLRBA.

The strong correlation between pAQP2-S269 and pLRBA (Fig. 1*A–C*) was consistent with screening results of a previous cross-linking mass spectrometry study, which showed that LRBA was in close proximity to AQP2 (27). LRBA was, indeed, expressed in renal collecting ducts, and it colocalized with AQP2 (Fig. 2*E* and *F*). Electron microscopy showed that both AQP2 and LRBA were localized at the intracellular vesicles in renal collecting ducts (Fig. 2*G*). Furthermore, double-label electron microscopy revealed that they were colocalized on the same vesicles (Fig. 2*H*).

Biallelic disease-causing mutations in *LRBA* abolish LRBA protein expression and cause a human immune dysregulation syndrome (28). However, it has been reported that *Lrba*$^{-/-}$ mice do not show immunological manifestations (29, 30). *Lrba*$^{-/-}$ mice, which we generated, also did not exhibit immunological phenotype, including hypogammaglobulinemia, organomegaly, and chronic diarrhea (*SI Appendix*, Fig. S4*A–C*). Moreover, no obvious renal impairment was detected in *Lrba*$^{-/-}$ mice. Lymphocytic infiltration, albuminuria, and serum creatinine elevation were not observed (*SI Appendix*, Fig. S4*D–G*).

Impaired Vasopressin-Induced AQP2 Phosphorylation in *Lrba*$^{-/-}$ Mice. LRBA is classified as an AKAP that interacts with PKA and other signaling molecules (17, 18, 31), thereby allowing the AKAP-anchored PKA to phosphorylate specific PKA substrates. We found that LRBA interacted especially with the PKA RIIβ subunit in vitro (Fig. 3*A*), in line with a similar finding in a B cell lymphoma cell line (18). The interaction between LRBA and PKA RIIβ was also observed at native expression levels (Fig. 3*B*). The upper band of LRBA (indicated by the arrow in Fig. 3*B*) was preferentially captured by PKA RIIβ in vivo. In renal collecting ducts, PKA directly phosphorylates AQP2-S256, which is critical for AQP2 activity and renal fluid retention (4, 6, 8). Therefore, we examined renal phenotypes of *Lrba*$^{-/-}$ mice. The baseline urine osmolality in *Lrba*$^{-/-}$ mice (1,317 ± 114 mOsm/kg (mean ± SD)) was lower than that in wild-type (WT) (2,804 ± 236 mOsm/kg) and *Lrba*$^{+/-}$ (2,574 ± 344 mOsm/kg) mice (Fig. 3*C*). As a result, *Lrba*$^{-/-}$ mice exhibited polyuria and polydipsia (Fig. 3*C*). Additionally, the maximal urine osmolality after water deprivation was reduced to 1,707 ± 134 mOsm/kg (mean ± SD) in *Lrba*$^{-/-}$ mice (maximal urine osmolality in WT mice, 3,708 ± 300 mOsm/kg (mean ± SD)), resulting in a rapid decline in body weight (Fig. 3*D* and *E*). Impaired urine-concentrating ability was caused by renal unresponsiveness to vasopressin (Fig. 3*F*). *Lrba*$^{-/-}$ mice showed only a slight increase in urine osmolality to 1,323 ± 362 mOsm/kg (mean ± SD), even after the administration of dDAVP (urine osmolality in WT mice, 3,027 ± 282 mOsm/kg (mean ± SD)).

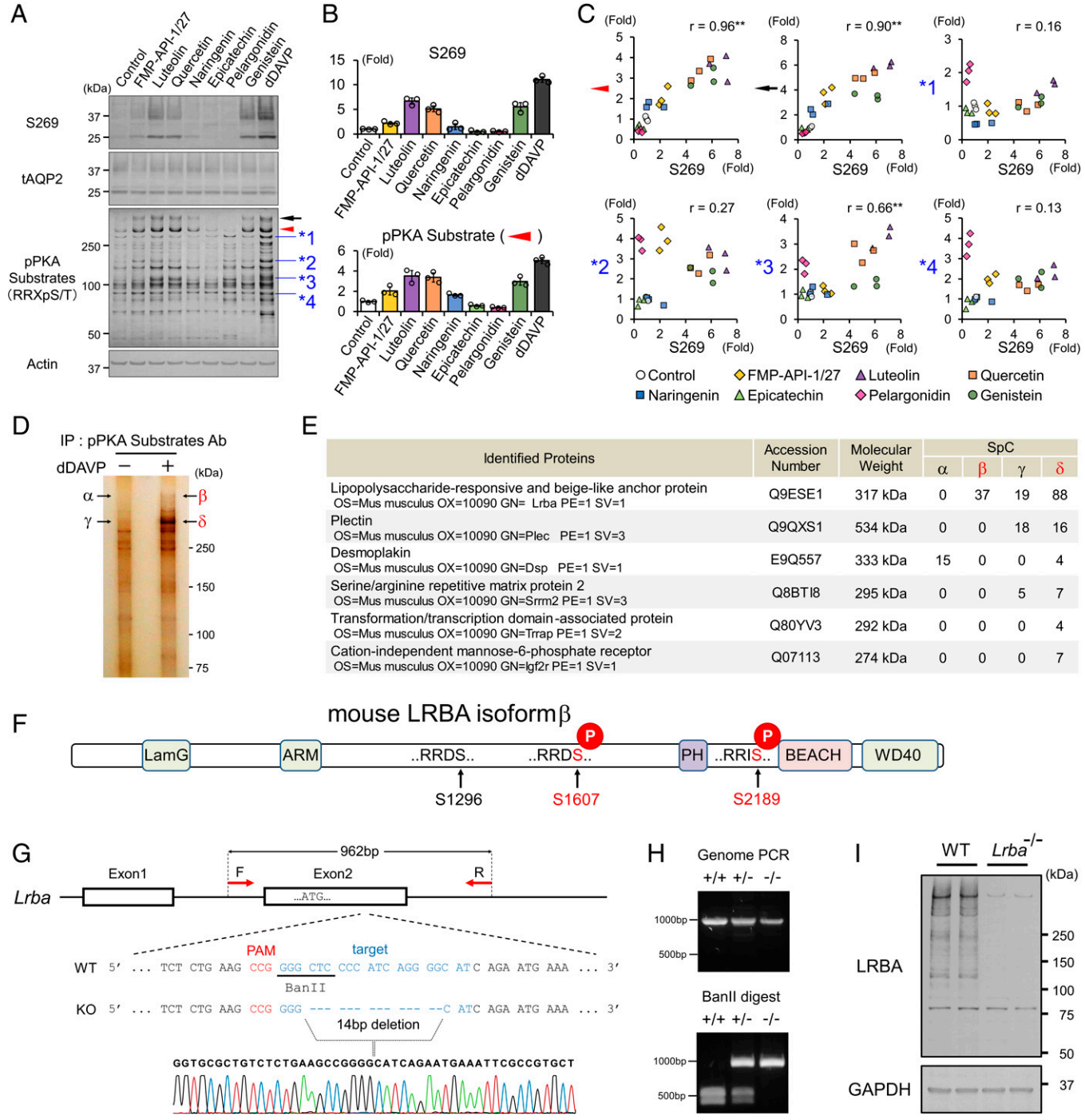

Identified Proteins	Accession Number	Molecular Weight	SpC			
			α	β	γ	δ
Lipopolysaccharide-responsive and beige-like anchor protein OS=Mus musculus OX=10090 GN= Lrba PE=1 SV=1	Q9ESE1	317 kDa	0	37	19	88
Plectin OS=Mus musculus OX=10090 GN=Plec PE=1 SV=3	Q9QXS1	534 kDa	0	0	18	16
Desmoplakin OS=Mus musculus OX=10090 GN=Dsp PE=1 SV=1	E9Q557	333 kDa	15	0	0	4
Serine/arginine repetitive matrix protein 2 OS=Mus musculus OX=10090 GN=Srrm2 PE=1 SV=3	Q8BTI8	295 kDa	0	0	5	7
Transformation/transcription domain-associated protein OS=Mus musculus OX=10090 GN=Trrap PE=1 SV=2	Q80YV3	292 kDa	0	0	0	4
Cation-independent mannose-6-phosphate receptor OS=Mus musculus OX=10090 GN=Igf2r PE=1 SV=1	Q07113	274 kDa	0	0	0	7

Fig. 1. FMP-API-1/27 and flavonoids phosphorylate LRBA and AQP2 in a correlated manner. (*A*–*C*) Screening for PKA substrates whose phosphorylation are well correlated with pAQP2-S269. (*A*) Representative blots of pAQP2-S269 and pPKA substrates. (*B*) Phosphorylation levels of AQP2-S269 and the PKA substrate (indicated by red arrowhead) are quantified by densitometric analysis ($n = 3$). (*C*) Phosphorylation levels of AQP2-S269 and PKA substrates (indicated by arrowheads) are strongly correlated in scatterplots. (*D* and *E*) Immunoprecipitated PKA substrates (indicated by β and δ) are identified as LRBA by liquid chromatography–tandem mass spectrometry (LC-MS/MS). (*D*) Representative silver staining of pPKA substrates immunoprecipitated by pPKA substrate antibody. (*E*) Identified proteins by LC-MS/MS. (*F*) PTM analysis reveals the RRXS sites of LRBA phosphorylated by dDAVP. (*G* and *H*) *Lrba* knockout mice are generated by CRISPR/Cas9 genome-editing technology. (*G*) The target sequence for *Lrba* gene editing. (*H*) Genotyping of *Lrba* knockout mice after BanII digestion of the PCR products from genomic DNA. (*I*) Anti-LRBA antibody detects renal LRBA in WT mice. (*C*) Pearson correlation coefficient *r* value and two-sided Student's *t* test. $^{**}P < 0.01$. Ab, antibody; IP, immunoprecipitation; PAM, protospacer adjacent motif; SpC, spectral count.

Vasopressin-dependent AQP2 phosphorylation is an essential determinant of urinary concentration. Total mRNA and protein expression of AQP2 were not different between WT and $Lrba^{-/-}$ mice (Fig. 4*A*–*C*). Importantly, phosphorylation at AQP2-S256 was unresponsive to dDAVP in $Lrba^{-/-}$ mice (Fig. 4*B* and *C*). pAQP2-S256 is necessary for downstream phosphorylation of other AQP2 serines, such as AQP2-S269 (6). In line with the impaired AQP2-S256 phosphorylation, AQP2-S269 in $Lrba^{-/-}$ mice was also not phosphorylated following dDAVP treatment (Fig. 4*B* and *C*).

pAQP2-S256 is physiologically important for promoting AQP2 exocytosis, whereas pAQP2-S269 reduces AQP2 endocytosis, leading to accumulation of pAQP2 at the apical plasma membrane (32). pAQP2-S269 is broadly accepted as a marker for AQP2 activation

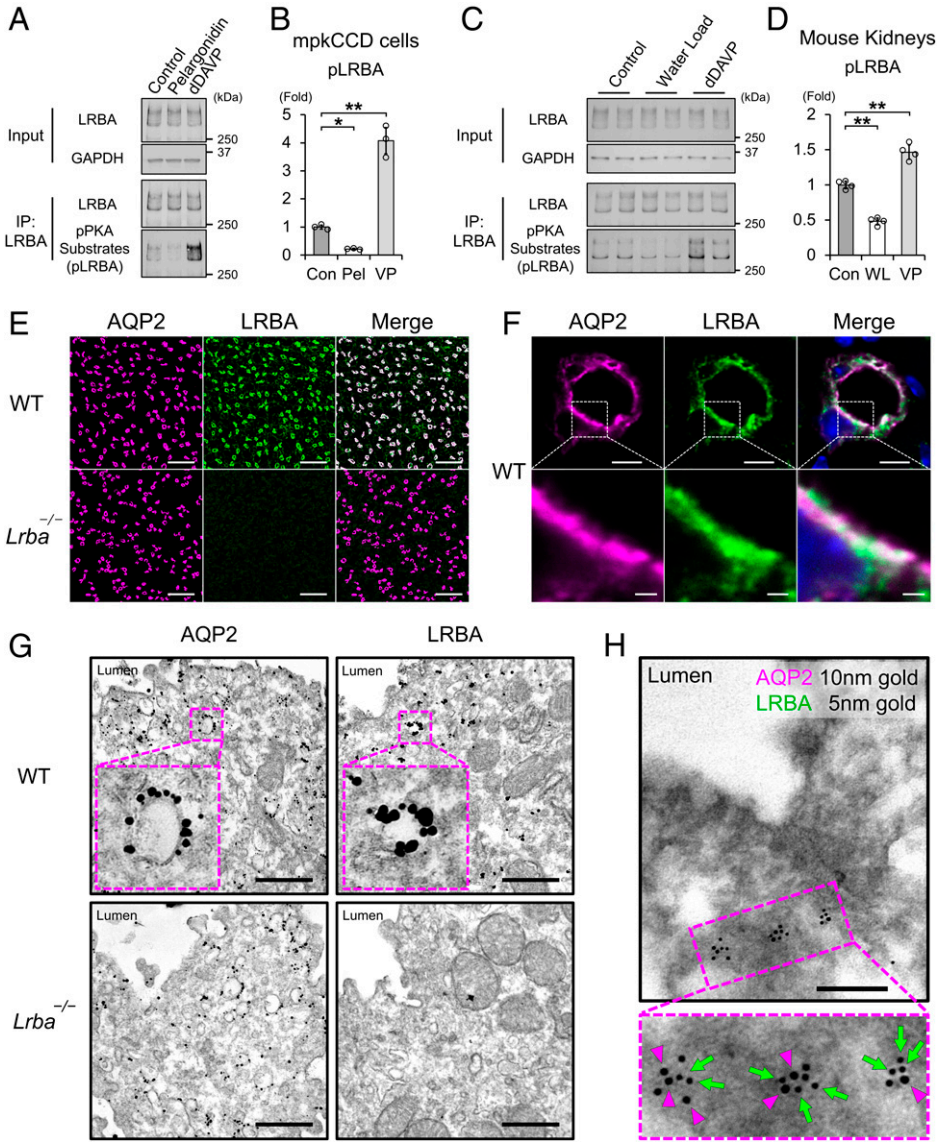

Fig. 2. LRBA colocalized with AQP2 at vesicles in the subapical region. (*A* and *B*) The effects of pelargonidin and vasopressin on LRBA phosphorylation in mpkCCD cells ($n = 3$). (*C* and *D*). The effects of water load and vasopressin on LRBA phosphorylation in vivo ($n = 4$). (*E* and *F*) Immunofluorescence staining showing that AQP2 (magenta) and LRBA (green) are colocalized in the kidneys of WT mice. (*E*) Scale bars, 100 μm. (*F*) Scale bars: top, 5 μm; bottom, 1 μm. (*G*) Immuno-electron microscopy showing that AQP2 and LRBA are localized at vesicles in renal collecting ducts of WT mice. Scale bars, 500 nm. (*H*) Colocalization of AQP2 and LRBA at the same intracellular vesicles. Double-label immuno-electron microscopy of AQP2 (10-nm gold indicated by magenta arrowheads) and LRBA (5-nm gold indicated by green arrows) in renal collecting ducts of WT mice. Scale bars, 200 nm. Data are reported as mean ± SD. $^{*}P < 0.05$, $^{**}p < 0.01$ by Dunnett's test. IP, immunoprecipitation; Pel, pelargonidin; VP, dDAVP; WL, water load.

because it is exclusively detected at the apical plasma membrane (9). Immunofluorescent analysis showed that most of the pAQP2-S256 and pAQP2-S269 were localized at the apical plasma membrane in WT mice by dDAVP stimulation (Fig. 4*D* and *E* and *SI Appendix*, Fig. S5*A–D*). Conversely, enhanced signal intensity of pAQP2-S256 and pAQP2-S269 by dDAVP stimulation was not observed in *Lrba*$^{-/-}$ mice. These results indicated that LRBA was crucial for AQP2 phosphorylation at S256 and S269, therefore leading to the defective AQP2 trafficking in *Lrba*$^{-/-}$ mice. Immunoelectron microscopy showed that dDAVP-induced AQP2 translocation to the apical plasma membrane was clearly impaired in *Lrba*$^{-/-}$ mice (Fig. 4*F*). AQP2-containing vesicles remained largely in the subapical region.

PKA Substrates Other Than AQP2 Phosphorylated in *Lrba*$^{-/-}$ Mice. *Lrba*$^{-/-}$ mice displayed elevated serum vasopressin levels, most likely as a compensatory mechanism in the face of water diuresis due to unphosphorylated AQP2 (Fig. 5*A*). As pPKA substrates were predominantly localized at collecting ducts but not at other renal tubules in the inner medulla (Fig. 5*B*), the inner medulla was dissected from mouse kidneys to investigate the effects of high vasopressin levels on PKA substrates in vivo. Increased vasopressin secretion by *Lrba* knockout mice led to strongly phosphorylated PKA substrates in the inner medullary collecting ducts (IMCDs), and their phosphorylation was further augmented by dDAVP administration (Fig. 5*C*). These results indicated that the vasopressin/cAMP/PKA signaling pathway phosphorylated a large number of PKA substrates in IMCDs, even in the absence of LRBA.

We further examined the effects of vasopressin on a PKA substrate localized at intracellular vesicles. In IMCDs, AQP2 and urea transporter A1 (UT-A1) coordinately regulate vasopressin-dependent urinary concentration (33). Membrane-trafficking mechanisms of UT-A1 have much in common with those of AQP2. Both UT-A1 and AQP2 contain RRXS motifs (*SI Appendix*, Fig. S6), and their translocation from intracellular

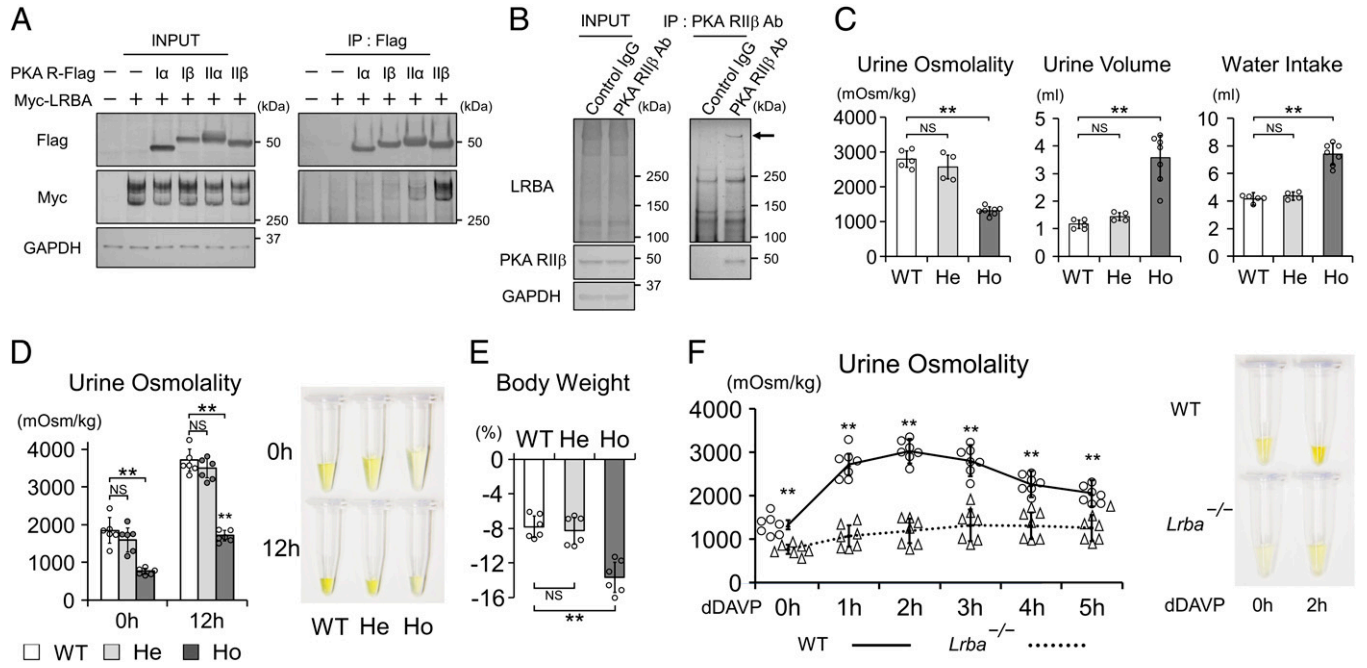

Fig. 3. *Lrba* knockout mice display the NDI phenotype. (*A*) LRBA interacts with PKA RIIα and RIIβ in vitro. FLAG-tagged PKA regulatory subunits and Myc-tagged LRBA were overexpressed in HEK293T cells. Anti-FLAG beads were used to perform coimmunoprecipitations. (*B*) LRBA interacts with PKA RIIβ in vivo. Membrane fraction of mouse kidneys was prepared. Anti-RIIβ antibody was used to perform a coimmunoprecipitation assay. (*C*) The baseline urine-concentrating ability is impaired in $Lrba^{-/-}$ mice. Metabolic cages were used to monitor urine osmolality, urine volume, and water intake for 24 h. ($n = 5$ WT mice; $n = 4$, He mice; $n = 7$ Ho mice). (*D* and *E*) The maximal urine-concentrating ability is impaired in $Lrba^{-/-}$ mice. Mice were deprived of water for 12 h. (*D*) *Left*, urine osmolality at the beginning and end of the experiments ($n = 6$). *Right*, representative urine samples. (*E*) Percentage of weight loss after water deprivation test ($n = 6$). (*F*) Urine osmolality of $Lrba^{-/-}$ mice is unresponsive to vasopressin. *Left*, changes in urine osmolality of WT and $Lrba^{-/-}$ mice after the treatment of dDAVP (0.4 μg/kg) ($n = 7$). *Right*, representative urine samples. (*C–E*) Data are reported as mean ± SD. $^{**}P < 0.01$, NS, not significant by Dunnett's test. (*F*) $^{**}P < 0.01$ by two-sided Student's *t* test. Ab, antibody; He, $Lrba^{+/-}$; Ho, $Lrba^{-/-}$; IP, immunoprecipitation.

vesicles to the apical plasma membrane are promoted in response to phosphorylation of RRXS motifs by PKA (34). Baseline UT-A1 protein expression was extremely high in $Lrba^{-/-}$ mice with vasopressin oversecretion (Fig. 5*D*) (35). This effect was reversed by a V2R antagonist, tolvaptan. Tolvaptan attenuated the PKA activity in IMCDs (Fig. 5*E* and *SI Appendix*, Fig. S7*A* and *B*), leading to a decrease in mRNA and protein expression of UT-A1 in $Lrba^{-/-}$ mice (Fig. 5*F* and *SI Appendix*, Fig. S8*A* and *B*). Despite similar subcellular distribution of AQP2 and UT-A1 (36), knockout of *Lrba* negatively influenced AQP2 but not UT-A1 phosphorylation (Fig. 5*G* and *H*). These results indicated that LRBA quite specifically mediated AQP2 phosphorylation in the renal vasopressin-signaling pathway.

The LRBA–PKA Interaction as a Drug Target for Urinary Concentration. In renal collecting ducts, dissociation of AKAP–PKA interactions by a low-molecular-weight compound, FMP-API-1/27, has been reported to result in strong phosphorylation of AQP2 (4, 37, 38); however, it has remained unclear which AKAP–PKA interaction was dissociated by FMP-API-1/27. Thus, we examined the dissociation of LRBA–PKA interaction. Overexpressed V2R successfully mediated dDAVP-induced PKA activation in HEK293T cells (*SI Appendix*, Fig. S9*A* and *B*). Remarkably, dDAVP almost totally dissociated the LRBA–PKA RIIβ interaction. FMP-API-1/27 possessed vasopressin-like effects and also dissociated the LRBA–PKA RIIβ interaction (Fig. 6*A*). Forskolin was used as a positive control for the activation of cAMP/PKA signaling pathway.

It is important to investigate the target specificity of FMP-API-1/27, because FMP-API-1/27 is a lead compound for increasing urine osmolality in an NDI mouse model with severe polyuria (37). Recent omics data provided information about AKAPs expressed in renal collecting ducts (Fig. 6*B*) (40–43). Aside from LRBA–PKA RIIβ interaction, FMP-API-1/27 only slightly inhibited the AKAP13–PKA RIIα interaction, whereas forskolin inhibited ARFGEF2–PKA RIIα, AKAP12–PKA RIIβ, MSN–PKA RIIβ, OPA1–PKA RIIα, and OPA1–PKA RIIβ interactions (Fig. 6*C* and *SI Appendix*, Fig. S10). These results indicated that FMP-API-1/27 was not a pan–AKAP–PKA interactions inhibitor, but rather specifically dissociated LRBA-anchored PKA, similar to vasopressin's effect.

Discussion

In the present study, we discovered that LRBA is indispensable for AQP2 phosphorylation in the vasopressin/cAMP/PKA signaling pathway in the urinary concentration system (Fig. 6*D*). We employed the innovative approach of generating phosphorylation patterns of PKA substrates using FMP-API-1/27 and several flavonoids to discover pathophysiologically important PKA substrates. From this, LRBA emerged as a leading candidate critical for AQP2 phosphorylation and a prime PKA substrate in mpkCCD cells whose phosphorylation correlated nearly perfectly with pAQP2-S269 (Fig. 1*A*). While, as an alternative, comprehensive phosphoproteomic analyses provide more detailed information about phosphorylation status, it is often challenging to narrow down and uncover a pathogenic PKA substrate with such analyses. Contrastingly, immunoprecipitation with pPKA substrate antibody is a rapid and cost-effective method, potentially applicable to extrarenal cell lines and organs for similar purposes.

While our screen focused on PKA substrates in mpkCCD cells, the primary hit, LRBA unexpectedly also had the property of an anchor protein (AKAP) that interacted with PKA (17, 18).

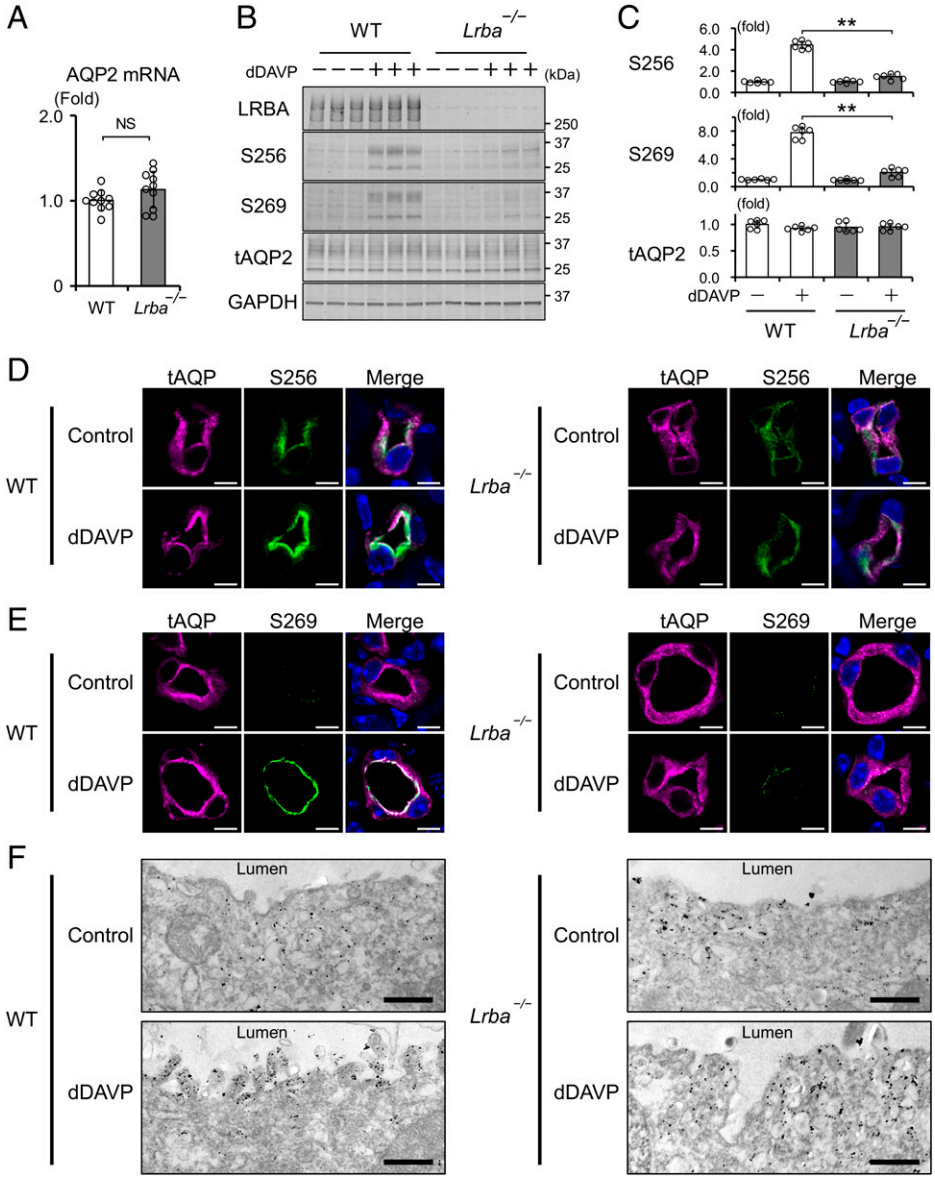

Fig. 4. *Lrba* knockout impairs AQP2 phosphorylation and trafficking. (*A*) AQP2 mRNA levels are not different between WT and *Lrba*$^{-/-}$ mice. AQP2 mRNA levels were quantified by qPCR ($n = 10$). (*B* and *C*) AQP2 phosphorylation is impaired in *Lrba*$^{-/-}$ mice. dDAVP (0.4 μg/kg) was intraperitoneally injected into WT and *Lrba*$^{-/-}$ mice for 1 h ($n = 6$). (*D* and *E*) Enhanced signal intensity of pAQP2-S256 and pAQP2-S269 by dDAVP is impaired in *Lrba*$^{-/-}$ mice. Immunofluorescence staining of AQP2 (magenta) and pAQP2-S256 (green) (*D*) or pAQP2-S269 (green) (*E*) in the kidneys of WT and *Lrba*$^{-/-}$ mice. dDAVP was administered as in *B*. Scale bars, 5 μm. (*F*) Immuno-electron microscopy showing that accumulation of AQP2 at the apical plasma membrane by dDAVP is impaired in *Lrba*$^{-/-}$ mice. dDAVP was administered as in *B*. Scale bars, 500 nm. Data are reported as mean ± SD. (*A*) Two-sided Student's *t* test. (*C*) $^{**}P < 0.01$ by Dunnett's test. NS, not significant.

The subcellular localization of PKA is usually determined by its AKAPs, and knockout of a single AKAP in vivo has been commonly used as a method to exclude PKA from each AKAP compartment (44, 45). Loss of LRBA–PKA complex from LRBA-containing vesicles in *Lrba* knockout mice led to a failure of AQP2 phosphorylation at residue S256 (Fig. 4*B–D*). Phosphorylation of AQP2-S256 by PKA is necessary for AQP2 translocation to the apical plasma membrane (32). Accordingly, *Lrba*$^{-/-}$ mice had water diuresis (Fig. 3*C*) and subsequent compensatory increase in serum vasopressin levels (Fig. 5*A*). Urine osmolality did not elevate even after the administration of exogenous vasopressin (Fig. 3*F*). Thus, LRBA served as an intermediary between PKA and AQP2 in the vasopressin signaling pathway. To achieve a strong correlation between AQP2 and LRBA phosphorylation (Fig. 1*A–C*), it was presumed that LRBA-anchored PKA simultaneously phosphorylated LRBA as well as AQP2. This autophosphorylation system in LRBA is not a specific phenomenon. Other AKAPs also contain multiple PKA recognition sequences (*SI Appendix*, Table S1), some of which are autophosphorylated by anchored PKA. As an example, AKAP12 is autophosphorylated by AKAP12-anchored PKA and regulates the binding affinity between AKAP12 and β2-adrenergic receptor (46). Such effects may reasonably be anticipated for LRBA-anchored PKA to indirectly modulate AQP2 activity.

The strength of AKAP–PKA interactions are individually different and dynamically modulated depending on the phosphorylation status at PKA. Only the RRXS motif present in PKA RII subunits is constitutively phosphorylated by PKA C subunits at basal conditions. For example, in cardiac cells, phosphorylation of this residue enhances binding affinity of PKA RII subunits to AKAP13 and AKAP15/18δ, facilitating the formation of AKAP–PKA complexes (47, 48). Contrarily,

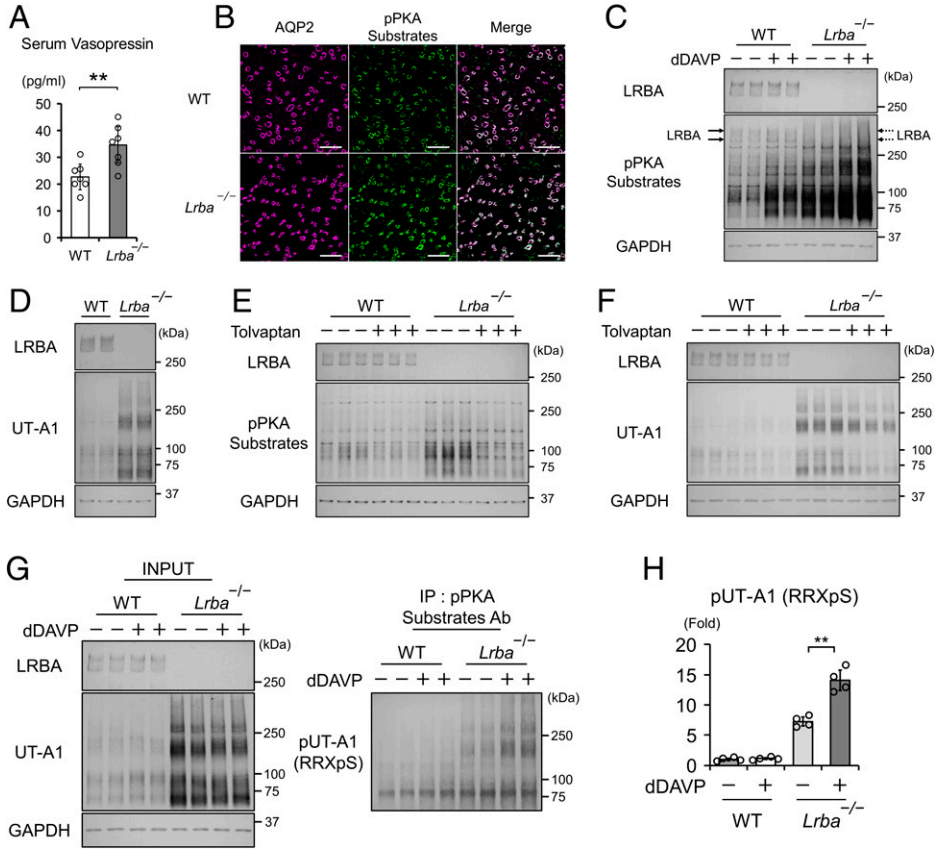

Fig. 5. Vasopressin phosphorylates most of the renal PKA substrates in *Lrba*$^{-/-}$ mice. (*A*) Serum vasopressin levels are elevated in *Lrba*$^{-/-}$ mice ($n = 3$ WT mice; $n = 4$ *Lrba*$^{-/-}$ mice). (*B*) pPKA substrates are localized at renal collecting ducts. Immunofluorescence staining of AQP2 (magenta) and pPKA substrates (green) in WT and *Lrba*$^{-/-}$ mice. Scale bars, 100 μm. (*C*) Vasopressin enhances phosphorylation of PKA substrates in *Lrba*$^{-/-}$ mice. dDAVP (0.4 μg/kg) was intraperitoneally administered into WT and *Lrba*$^{-/-}$ mice for 1 h ($n = 6$). (*D*) Protein expression of UT-A1 is increased in *Lrba*$^{-/-}$ mice ($n = 6$). (*E*) Tolvaptan suppresses PKA activity in *Lrba*$^{-/-}$ mice. WT and *Lrba*$^{-/-}$ mice were subcutaneously infused with tolvaptan (25 mg/kg/d) for 48 h using osmotic minipumps ($n = 6$). (*F*) Tolvaptan decreases protein expressions of UT-A1. Mice were administered tolvaptan as in *E* ($n = 5$). (*G*) UT-A1 is phosphorylated by vasopressin in *Lrba*$^{-/-}$ mice. At 1 h after the administration of dDAVP (0.4 μg/kg), UT-A1 was immunoprecipitated by a pPKA-substrate antibody and probed with anti–UT-A1 antibody. (*H*) Densitometric analysis of pUT-A1 ($n = 4$). Data are reported as mean ± SD. (*A*) $^{**}P < 0.01$ by two-sided Student's *t* test. (*H*) $^{**}P < 0.01$ by Tukey test. (*C*–*H*) The inner medulla was dissected from the kidneys. Ab, antibody; IP, immunoprecipitation.

LRBA–PKA RIIβ, AKAP12–PKA RIIβ, MSN–PKA RIIβ, and OPA1–PKA RIIβ interactions were readily dissociated by forskolin (Fig. 6*A* and *C* and *SI Appendix*, Fig. S10), despite significant phosphorylation at the RRXS site in PKA RIIβ (*SI Appendix*, Fig. S11). Vasopressin behaved as an AKAP–PKA interaction inhibitor, at least for the LRBA–PKA interaction (*SI Appendix*, Fig. S9*A* and *B*), releasing the active form of PKA from LRBA. In renal collecting ducts, dissociation of AKAP–PKA interactions is an emerging therapeutic strategy for the phosphorylation of AQP2 in the treatment of intractable polyuria (4, 37). Notably, among various AKAP–PKA interactions, the LRBA–PKA interaction was specifically dissociated by an AQP2 activator, FMP-API-1/27 (Fig. 6*A*–*C*). Based on these results, we speculate that the action range of LRBA-anchored PKA was restricted by the LRBA–PKA interaction under resting conditions, resulting in the suppression of PKA activity, whereas PKA unanchored by vasopressin or FMP-API-1/27 acquired kinase activity, which presumably enhanced AQP2 phosphorylation.

The LRBA-anchored PKA is a potential drug target for AQP2 phosphorylation and urinary concentration. One of the limitations of FMP-API-1/27 is that it was ineffective for diabetes insipidus with AQP2 deficiency. We generated a lithium-induced diabetes insipidus mouse model. In line with previous reports (49), lithium chloride decreased AQP2 protein expression levels, leading to low urine osmolality (*SI Appendix*, Fig. S12*A* and *B*). However, the amount of AQP2 was quite low, so that phosphorylation of AQP2-S256 and AQP2-S269 by FMP-API-1/27 was not detected. Our prior study revealed that AQP2 protein expression was not increased by FMP-API-1/27 (37). Specific activation of LRBA-anchored PKA by FMP-API-1/27 was insufficient to improve urine osmolality in the case of AQP2 deficiency. It has been reported that basal expression levels of AQP2 are not reduced in some of the congenital NDI mouse models with V2R mutations (50). LRBA–PKA interaction inhibitors may effectively improve urine-concentrating ability of NDI mouse models without AQP2 deficiency.

Imperfect specificity of the pPKA substrate antibody is another limitation of this study. It has been noted that the RRXS/T motif is phosphorylated by not only PKA but also a lot of other kinases, including protein kinase G and protein kinase C in the AGC kinase group (51). Importantly, these kinases take part in AQP2 phosphorylation (52–54). Although we used a direct PKA activator, FMP-API-1/27, to exclude the effects of these kinases on phosphorylation of RRXS/T sites, the responsible kinase was not specified by the pPKA substrate antibody. PKA-independent phosphorylation of RRXS sites might explain bands in Fig. 1*A* (indicated by blue asterisks) whose phosphorylation levels were not correlated with those of AQP2-S269.

In addition to RRXS, PKA can phosphorylate other targets with R in position −3 relative to the phosphorylation site, such as RKXS. Although LRBA contains several RRXS and RKXS sequences, the pPKA substrate antibody cannot distinguish

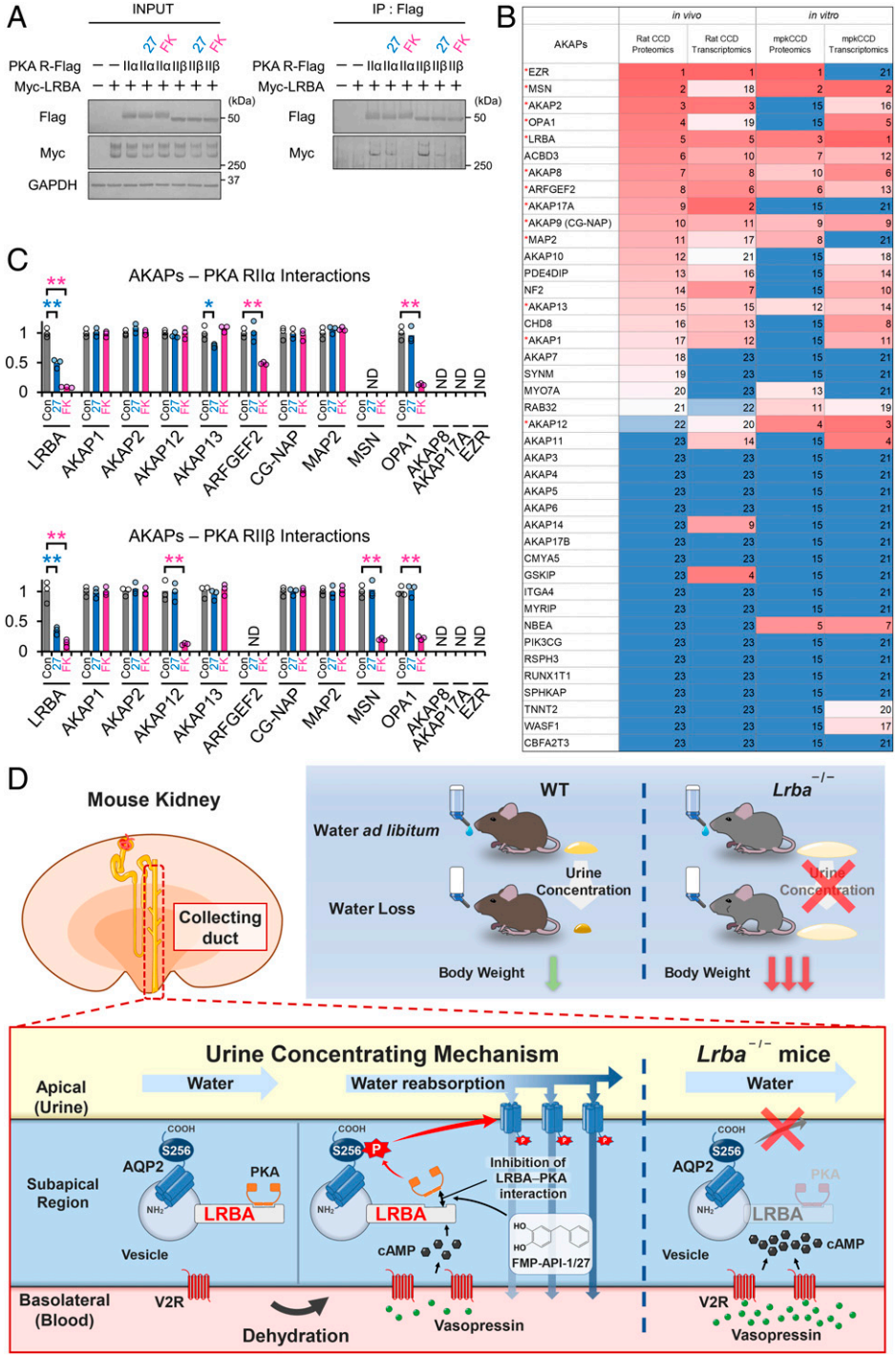

AKAPs	in vivo: Rat CCD Proteomics	in vivo: Rat CCD Transcriptomics	in vitro: mpkCCD Proteomics	in vitro: mpkCCD Transcriptomics
*EZR	1	1	1	21
*MSN	2	18	2	2
*AKAP2	3	3	15	16
*OPA1	4	19	15	5
*LRBA	5	5	3	1
ACBD3	6	10	7	12
*AKAP8	7	8	10	6
*ARFGEF2	8	6	6	13
*AKAP17A	9	2	15	21
*AKAP9 (CG-NAP)	10	11	9	9
*MAP2	11	17	8	21
AKAP10	12	21	15	18
PDE4DIP	13	16	15	14
NF2	14	7	15	10
*AKAP13	15	15	12	14
CHD8	16	13	15	8
*AKAP1	17	12	15	11
AKAP7	18	23	15	21
SYNM	19	23	15	21
MYO7A	20	23	13	21
RAB32	21	22	11	19
*AKAP12	22	20	4	3
AKAP11	23	14	15	4
AKAP3	23	23	15	21
AKAP4	23	23	15	21
AKAP5	23	23	15	21
AKAP6	23	23	15	21
AKAP14	23	9	15	21
AKAP17B	23	23	15	21
CMYA5	23	23	15	21
GSKIP	23	4	15	21
ITGA4	23	23	15	21
MYRIP	23	23	15	21
NBEA	23	23	5	7
PIK3CG	23	23	15	21
RSPH3	23	23	15	21
RUNX1T1	23	23	15	21
SPHKAP	23	23	15	21
TNNT2	23	23	15	20
WASF1	23	23	15	17
CBFA2T3	23	23	15	21

Fig. 6. The LRBA–PKA interaction is the drug target of FMP-API-1/27. (*A*) FMP-API-1/27 dissociates the LRBA–PKA RIIβ interaction. PKA RII subunits (RIIα, RIIβ)-Flag and Myc-LRBA were overexpressed in HEK293T cells. FMP-API-1/27 (200 μM) or forskolin (10 μM) was added to the cells 1 h before coimmunoprecipitation. Representative blots of coimmunoprecipitated Myc-LRBA are shown ($n = 3$). (*B*) Highly expressed AKAP proteins and mRNA in renal collecting ducts are listed based on recent omics data (39–43). Expression levels are indicated by a color scale, with red representing relative high expression levels and blue indicating relative low expression levels. The numbers in the table indicate rank in sequential order. Highly expressed AKAPs, which are evaluated in *C* and *SI Appendix*, Fig. S10, are indicated by red asterisks. (*C*) FMP-API-1/27 and forskolin inhibit specific AKAP–PKA interactions. A coimmunoprecipitation assay for measuring AKAP–PKA interactions (*SI Appendix*, Fig. S10) was performed as in *A*. Densitometric analysis of coimmunoprecipitated AKAPs ($n = 3$). (*D*) Schematic summary of the physiological role of LRBA in the urine-concentrating system. *Lrba*$^{-/-}$ mice exhibited polyuria, and their urine-concentrating ability did not respond to vasopressin. As a result of diluted urine, serum vasopressin levels were elevated to compensate for water loss in *Lrba*$^{-/-}$ mice. Exclusion of PKA from the LRBA compartment by *Lrba* knockout caused a failure of PKA-induced AQP2 phosphorylation. The strength of LRBA–PKA interaction was dynamically changed by AQP2 activators. Vasopressin and FMP-API-1/27 dissociated PKA from LRBA, presumably to enhance AQP2 phosphorylation at S256. (*C*) Mean data are reported. $^{**}P < 0.05$, $^{*}P < 0.01$ by Tukey test. IP, immunoprecipitation; ND, AKAP–PKA interactions not detected.

phosphorylation status of individual sites. Interestingly, PTM analysis of LRBA protein showed that RKDS^{979} and RKVT^{1669} were dephosphorylated by dDAVP (*SI Appendix*, Fig. S2*B*). Isobe et al. (10) reported similar results. In the PKA-null mpkCCD cell lines, phosphorylation of RKDS^{979} is increased (10). The PKA-independent signaling pathway may regulate dephosphorylation of RKDS^{979} and RKVT^{1669} in the vasopressin-signaling pathway.

Most of the biallelic pathogenic mutations in *LRBA* cause absence of LRBA protein expression in peripheral blood mononuclear cells, causing immune system pathologies (55). Irrespective of the locations and types of mutations in *LRBA*, mutation-derived unstable mRNA or misfolded protein may be mostly degraded, thereby contributing to LRBA deficiency (55). Severe reduction of LRBA protein expression may be taking place in the kidneys of patients; however, polyuric phenotype of LRBA deficiency has not been reported. Urine osmolality of $Lrba^{-/-}$ mice was higher than that of *Avpr2* (V2R) knockout mice, and thus $Lrba^{-/-}$ mice were not neonatal lethal, as opposed to $Avpr2^{-/-}$ mice. Residual AKAPs–PKA complexes, such as AKAP220–PKA and AKAP7δ–PKA, may compensate for AQP2 phosphorylation in response to elevated serum vasopressin levels (Fig. 5*A*). AKAP220 and AKAP7δ expression levels remained unchanged in $Lrba^{-/-}$ mice (*SI Appendix*, Fig. S13*A* and *B*). Furthermore, excessive serum vasopressin presumably activated PKA-independent vasopressin signaling in renal collecting ducts. AQP2-S256 is partially phosphorylated by vasopressin even in PKA-null mpkCCD cell lines through activation of potential candidate kinases, including SNF1-subfamily kinases, Prkci (an atypical protein kinase C), and protein kinase G (56). These kinases may contribute to PKA-independent AQP2 phosphorylation and mild polyuric phenotype of $Lrba^{-/-}$ mice. Remarkably, chronic kidney disease is not a rare complication in patients with LRBA deficiency (19, 57, 58). Taylan et al. (57) reported the case of a 6-y-old male patient whose renal function was impaired without proteinuria and edema during the assessment of his chronic diarrhea. Chronic diarrhea characterized by duodenal villous atrophy and large bowel lymphocytic infiltration is a common symptom of LRBA deficiency (59). Impaired urine-concentrating ability in combination with chronic diarrhea exacerbates the risk of rapid weight loss by dehydration (Fig. 3*E*), leading to chronic kidney disease (60). Therefore, body-fluid management may be required to avoid dehydration in LRBA deficiency.

In conclusion, we show that LRBA is necessary for the maintenance of body-water homeostasis. LRBA is a PKA-anchoring protein that is crucial for urinary concentration. LRBA mediates vasopressin-induced AQP2 phosphorylation in renal collecting ducts. $Lrba^{-/-}$ mice demonstrated resistance of AQP2 phosphorylation to vasopressin and exhibited polyuria.

Materials and Methods

See *SI Appendix* for full description of the materials and methods.

Study Approvals. All animal studies were performed in accordance with the guidelines for animal research of Tokyo Medical and Dental University. The study protocol was approved by the Animal Care and Use Committee of Tokyo Medical and Dental University (approval no. A2021-120C).

Animals. C57BL/6J female mice were used for experiments at age 10 wk. All mice were maintained under standard lightning conditions (12 h:12 h light-dark cycle).

Generation of *Lrba* Knockout Mice. *Lrba* knockout mice were generated in C57/BL6J zygotes using the CRISPR/Cas9 genome-editing system. This mutation led to a frameshift in *Lrba* transcript, resulting in the truncation of the LRBA protein.

Cell Culture. The mpkCCDcl4 cells were seeded and grown on semipermeable filters (Transwell, 0.4-μm pore size; Corning Coster). The mpkCCD cells were cultured for 5 d, with daily changes of the medium. HEK293T cells were cultured in 6-cm diameter dishes in Dulbecco's modified Eagle's medium supplemented with 10% fetal bovine serum.

Generation of Anti-LRBA Antibody. *Escherichia coli* BL21 (DE3) was transformed with the plasmid of GST-mouse LRBA (amino acid 1555–1795), and the GST fusion protein was generated. After cleavage of GST, rabbits were immunized by this protein to generate LRBA antibody.

Statistics. At least three independent experiments were performed to ensure reproducibility. Statistical analyses were performed with JMP14 software (SAS Institute, Inc.) using the two-sided Student's *t* test, Dunnett's test, Tukey test, or Pearson's correlation analysis. Statistical tests of each experiment are reported in the figure legends.

Data Availability. All raw liquid chromatography–tandem mass spectrometry data were deposited with the ProteomeXchange Consortium via the PRIDE (61) partner repository with the dataset identifiers PXD033852 (62) and PXD033859 (63). All other data are included in the manuscript and/or *SI Appendix*. *Lrba* knockout mice generated during this study are available from Fuminori Tokunaga (email: ftokunaga@omu.ac.jp), and anti-LRBA antibody generated during the study is available from Fumiaki Ando (email: fandkidc@tmd.ac.jp) on reasonable request.

ACKNOWLEDGMENTS. This work was supported by Grants-in-Aid for Scientific Research (B) (Grant 21H02933 to F.A.) and Scientific Research (A) (Grant 19H01049 to S.U.) from the Japan Society for the Promotion of Science; a Health Labour Science Research Grant from the Ministry of Health Labour and Welfare; the Japan Agency for Medical Research and Development (AMED) under Grant JP19ek0109304 and JP19lm0203023 to S.U.; and grants from the following to F.A.: Tokyo Medical and Dental University (TMDU) priority research areas grant, TMDU Young Innovative Medical Scientist Unit, The Uehara Memorial Foundation, Takeda Science Foundation, Pharmacodynamics Research Foundation, Japan Intractable Diseases (Nanbyo) Research Foundation (Grant 2018A01), MSD Life Science Foundation, and Public Interest Incorporated Foundation.

Author affiliations: [a]Department of Nephrology, Tokyo Medical and Dental University, Tokyo 113-8510, Japan; [b]Department of Medical Biochemistry, Graduate School of Medicine, Osaka Metropolitan University, Osaka 545-8585, Japan; [c]Department of Anatomy and Life Structure, Juntendo University Graduate School of Medicine, Tokyo 113-8421, Japan; [d]Research Core, Tokyo Medical and Dental University, Tokyo 113-8510, Japan; [e]Institute of Biomaterials and Bioengineering, Tokyo Medical and Dental University, Tokyo 101-0062, Japan; [f]Faculty of Pharmaceutical Sciences, Teikyo Heisei University, Tokyo 164-8530, Japan; [g]Advanced Research Institute, Tokyo Medical and Dental University, Tokyo 113-8501, Japan; and [h]Cellular and Structural Physiology Industrious Agency, 2-1-1, Otemachi, Chiyoda-ku, Tokyo 100-0004, Japan

Author contributions: F.A. and S.U. designed research; Y.H., F.A., D.O., K.I., H.Y., Y.S., A.N., and F.T. performed research; Y.H., F.A., D.O., T.F., S. Mori, M.T., H.K., and F.T. contributed new reagents/analytic tools; Y.H., F.A., S. Suzuki, N.Y., S. Mandai, K.S., T.M., E.S., T.R., S. Sasaki, and S.U. analyzed data; and Y.H. and F.A. wrote the paper.

1. J. M. Sands, D. G. Bichet, A. C. Physicians, A. P. Society; American College of Physicians; American Physiological Society, Nephrogenic diabetes insipidus. *Ann. Intern. Med.* **144**, 186–194 (2006).
2. H. B. Moeller, S. Rittig, R. A. Fenton, Nephrogenic diabetes insipidus: Essential insights into the molecular background and potential therapies for treatment. *Endocr. Rev.* **34**, 278–301 (2013).
3. M. Fujimoto *et al.*, Clinical overview of nephrogenic diabetes insipidus based on a nationwide survey in Japan. *Yonago Acta Med.* **57**, 85–91 (2014).
4. F. Ando, Activation of AQP2 water channels by protein kinase A: Therapeutic strategies for congenital nephrogenic diabetes insipidus. *Clin. Exp. Nephrol.* **25**, 1051–1056 (2021).
5. F. D. Smith *et al.*, Local protein kinase A action proceeds through intact holoenzymes. *Science* **356**, 1288–1293 (2017).
6. J. D. Hoffert *et al.*, Vasopressin-stimulated increase in phosphorylation at Ser269 potentiates plasma membrane retention of aquaporin-2. *J. Biol. Chem.* **283**, 24617–24627 (2008).
7. K. Fushimi, S. Sasaki, F. Marumo, Phosphorylation of serine 256 is required for cAMP-dependent regulatory exocytosis of the aquaporin-2 water channel. *J. Biol. Chem.* **272**, 14800–14804 (1997).
8. K. Eto, Y. Noda, S. Horikawa, S. Uchida, S. Sasaki, Phosphorylation of aquaporin-2 regulates its water permeability. *J. Biol. Chem.* **285**, 40777–40784 (2010).
9. H. B. Moeller, M. A. Knepper, R. A. Fenton, Serine 269 phosphorylated aquaporin-2 is targeted to the apical membrane of collecting duct principal cells. *Kidney Int.* **75**, 295–303 (2009).
10. K. Isobe *et al.*, Systems-level identification of PKA-dependent signaling in epithelial cells. *Proc. Natl. Acad. Sci. U.S.A.* **114**, E8875–E8884 (2017).
11. M. S. Kapiloff, M. Rigatti, K. L. Dodge-Kafka, Architectural and functional roles of A kinase-anchoring proteins in cAMP microdomains. *J. Gen. Physiol.* **143**, 9–15 (2014).
12. O. Torres-Quesada, J. E. Mayrhofer, E. Stefan, The many faces of compartmentalized PKA signalosomes. *Cell. Signal.* **37**, 1–11 (2017).

13. R. Okutsu *et al.*, AKAP220 colocalizes with AQP2 in the inner medullary collecting ducts. *Kidney Int.* **74**, 1429–1433 (2008).
14. E. Stefan *et al.*, Compartmentalization of cAMP-dependent signaling by phosphodiesterase-4D is involved in the regulation of vasopressin-mediated water reabsorption in renal principal cells. *J. Am. Soc. Nephrol.* **18**, 199–212 (2007).
15. B. W. Jones *et al.*, Cardiomyocytes from AKAP7 knockout mice respond normally to adrenergic stimulation. *Proc. Natl. Acad. Sci. U.S.A.* **109**, 17099–17104 (2012).
16. J. L. Whiting *et al.*, AKAP220 manages apical actin networks that coordinate aquaporin-2 location and renal water reabsorption. *Proc. Natl. Acad. Sci. U.S.A.* **113**, E4328–E4337 (2016).
17. J. W. Wang, J. Howson, E. Haller, W. G. Kerr, Identification of a novel lipopolysaccharide-inducible gene with key features of both A kinase anchor proteins and chs1/beige proteins. *J. Immunol.* **166**, 4586–4595 (2001).
18. N. C. Moreno-Corona *et al.*, Lipopolysaccharide-responsive beige-like anchor acts as a cAMP-dependent protein kinase anchoring protein in B cells. *Scand. J. Immunol.* **92**, e12922 (2020).
19. B. Lo *et al.*, AUTOIMMUNE DISEASE. Patients with LRBA deficiency show CTLA4 loss and immune dysregulation responsive to abatacept therapy. *Science* **349**, 436–440 (2015).
20. D. M. Sansom, IMMUNOLOGY. Moving CTLA-4 from the trash to recycling. *Science* **349**, 377–378 (2015).
21. W. C. Ko, C. M. Shih, Y. H. Lai, J. H. Chen, H. L. Huang, Inhibitory effects of flavonoids on phosphodiesterase isozymes from guinea pig and their structure-activity relationships. *Biochem. Pharmacol.* **68**, 2087–2094 (2004).
22. F. Orallo, M. Camiña, E. Alvarez, H. Basaran, C. Lugnier, Implication of cyclic nucleotide phosphodiesterase inhibition in the vasorelaxant activity of the citrus-fruits flavonoid (+/-)-naringenin. *Planta Med.* **71**, 99–107 (2005).
23. U. R. Kuppusamy, N. P. Das, Effects of flavonoids on cyclic AMP phosphodiesterase and lipid mobilization in rat adipocytes. *Biochem. Pharmacol.* **44**, 1307–1315 (1992).
24. C. Göttel *et al.*, In vitro inhibition of phosphodiesterase 3B (PDE 3B) by anthocyanin-rich fruit juice extracts and selected anthocyanins. *Int. J. Mol. Sci.* **21**, 6934 (2020).
25. M. Bens *et al.*, Corticosteroid-dependent sodium transport in a novel immortalized mouse collecting duct principal cell line. *J. Am. Soc. Nephrol.* **10**, 923–934 (1999).
26. U. Hasler *et al.*, Long term regulation of aquaporin-2 expression in vasopressin-responsive renal collecting duct principal cells. *J. Biol. Chem.* **277**, 10379–10386 (2002).
27. C. L. Chou *et al.*, Identification of UT-A1- and AQP2-interacting proteins in rat inner medullary collecting duct. *Am. J. Physiol. Cell Physiol.* **314**, C99–C117 (2018).
28. S. Habibi *et al.*, Clinical, immunologic, and molecular spectrum of patients with LPS-responsive beige-like anchor protein deficiency: A systematic review. *J. Allergy Clin. Immunol. Pract.* **7**, 2379–2386.e5 (2019).
29. D. L. Burnett, I. A. Parish, E. Masle-Farquhar, R. Brink, C. C. Goodnow, Murine LRBA deficiency causes CTLA-4 deficiency in Tregs without progression to immune dysregulation. *Immunol. Cell Biol.* **95**, 775–788 (2017).
30. L. Gámez-Díaz *et al.*, Immunological phenotype of the murine Lrba knockout. *Immunol. Cell Biol.* **95**, 789–802 (2017).
31. T. Hou, Y. Li, W. Wang, Prediction of peptides binding to the PKA RIIalpha subunit using a hierarchical strategy. *Bioinformatics* **27**, 1814–1821 (2011).
32. H. B. Moeller, J. Praetorius, M. R. Rützler, R. A. Fenton, Phosphorylation of aquaporin-2 regulates its endocytosis and protein-protein interactions. *Proc. Natl. Acad. Sci. U.S.A.* **107**, 424–429 (2010).
33. R. A. Fenton, M. A. Knepper, Urea and renal function in the 21st century: Insights from knockout mice. *J. Am. Soc. Nephrol.* **18**, 679–688 (2007).
34. M. A. Blount *et al.*, Phosphorylation of UT-A1 urea transporter at serines 486 and 499 is important for vasopressin-regulated activity and membrane accumulation. *Am. J. Physiol. Renal Physiol.* **295**, F295–F299 (2008).
35. Q. Cai *et al.*, Vasopressin increases expression of UT-A1, UT-A3, and ER chaperone GRP78 in the renal medulla of mice with a urinary concentrating defect. *Am. J. Physiol. Renal Physiol.* **299**, F712–F719 (2010).
36. J. M. Sands, M. A. Blount, J. D. Klein, Regulation of renal urea transport by vasopressin. *Trans. Am. Clin. Climatol. Assoc.* **122**, 82–92 (2011).
37. F. Ando *et al.*, AKAPs-PKA disruptors increase AQP2 activity independently of vasopressin in a model of nephrogenic diabetes insipidus. *Nat. Commun.* **9**, 1411 (2018).
38. F. Christian *et al.*, Small molecule AKAP-protein kinase A (PKA) interaction disruptors that activate PKA interfere with compartmentalized cAMP signaling in cardiac myocytes. *J. Biol. Chem.* **286**, 9079–9096 (2011).
39. C. R. Yang *et al.*, Deep proteomic profiling of vasopressin-sensitive collecting duct cells. I. Virtual Western blots and molecular weight distributions. *Am. J. Physiol. Cell Physiol.* **309**, C785–C798 (2015).
40. M. J. Yu *et al.*, Systems-level analysis of cell-specific AQP2 gene expression in renal collecting duct. *Proc. Natl. Acad. Sci. U.S.A.* **106**, 2441–2446 (2009).
41. J. W. Lee, C. L. Chou, M. A. Knepper, Deep sequencing in microdissected renal tubules identifies nephron segment-specific transcriptomes. *J. Am. Soc. Nephrol.* **26**, 2669–2677 (2015).
42. K. Limbutara, C. L. Chou, M. A. Knepper, Quantitative proteomics of all 14 renal tubule segments in rat. *J. Am. Soc. Nephrol.* **31**, 1255–1266 (2020).
43. N. K. Verma, M. L. S. Chalasani, J. D. Scott, D. Kelleher, CG-NAP/kinase interactions fine-tune T cell functions. *Front. Immunol.* **10**, 2642 (2019).
44. M. Weisenhaus *et al.*, Mutations in AKAP5 disrupt dendritic signaling complexes and lead to electrophysiological and behavioral phenotypes in mice. *PLoS One* **5**, e10325 (2010).
45. B. W. Jones *et al.*, Targeted deletion of AKAP7 in dentate granule cells impairs spatial discrimination. *eLife* **5**, e20695 (2016).
46. J. Tao, H. Y. Wang, C. C. Malbon, Protein kinase A regulates AKAP250 (gravin) scaffold binding to the beta2-adrenergic receptor. *EMBO J.* **22**, 6419–6429 (2003).
47. D. R. Zakhary, C. S. Moravec, M. Bond, Regulation of PKA binding to AKAPs in the heart: Alterations in human heart failure. *Circulation* **101**, 1459–1464 (2000).
48. S. Manni, J. H. Mauban, C. W. Ward, M. Bond, Phosphorylation of the cAMP-dependent protein kinase (PKA) regulatory subunit modulates PKA-AKAP interaction, substrate phosphorylation, and calcium signaling in cardiac cells. *J. Biol. Chem.* **283**, 24145–24154 (2008).
49. M. Christ-Crain *et al.*, Diabetes insipidus. *Nat. Rev. Dis. Primers* **5**, 54 (2019).
50. J. Yun *et al.*, Generation and phenotype of mice harboring a nonsense mutation in the V2 vasopressin receptor gene. *J. Clin. Invest.* **106**, 1361–1371 (2000).
51. N. Sugiyama, H. Imamura, Y. Ishihama, Large-scale discovery of substrates of the human kinome. *Sci. Rep.* **9**, 10503 (2019).
52. R. Bouley *et al.*, Nitric oxide and atrial natriuretic factor stimulate cGMP-dependent membrane insertion of aquaporin 2 in renal epithelial cells. *J. Clin. Invest.* **106**, 1115–1126 (2000).
53. D. Brown, U. Hasler, P. Nunes, R. Bouley, H. A. Lu, Phosphorylation events and the modulation of aquaporin 2 cell surface expression. *Curr. Opin. Nephrol. Hypertens.* **17**, 491–498 (2008).
54. P. W. Cheung, R. Bouley, D. Brown, Targeting the trafficking of kidney water channels for therapeutic benefit. *Annu. Rev. Pharmacol. Toxicol.* **60**, 175–194 (2020).
55. L. Gámez-Díaz *et al.*, The extended phenotype of LPS-responsive beige-like anchor protein (LRBA) deficiency. *J. Allergy Clin. Immunol.* **137**, 223–230 (2016).
56. A. Datta *et al.*, PKA-independent vasopressin signaling in renal collecting duct. *FASEB J.* **34**, 6129–6146 (2020).
57. C. Taylan *et al.*, Case report: Exome sequencing reveals LRBA deficiency in a patient with end-stage renal disease. *Front Pediatr.* **8**, 42 (2020).
58. F. Schreiner *et al.*, Infancy-onset T1DM, short stature, and severe immunodysregulation in two siblings with a homozygous LRBA mutation. *J. Clin. Endocrinol. Metab.* **101**, 898–904 (2016).
59. G. Azizi *et al.*, New therapeutic approach by sirolimus for enteropathy treatment in patients with LRBA deficiency. *Eur. Ann. Allergy Clin. Immunol.* **49**, 235–239 (2017).
60. C. Roncal-Jimenez, M. A. Lanaspa, T. Jensen, L. G. Sanchez-Lozada, R. J. Johnson, Mechanisms by which dehydration may lead to chronic kidney disease. *Ann. Nutr. Metab.* **66** (suppl. 3), 10–13 (2015).
61. Y. Perez-Riverol *et al.*, The PRIDE database resources in 2022: A hub for mass spectrometry-based proteomics evidences. *Nucleic Acids Res.* **50**, D543–D552 (2022).
62. Y. Hara and S.Uchida, cAMP/PKA signaling phosphorylates LRBA in renal collecting duct, PRIDE, https://www.ebi.ac.uk/pride/archive/projects/PXD033852. Deposited 12 May 2022.
63. Y. Hara and S.Uchida, Mass spectrometry-based analysis of LRBA phosphorylation, PRIDE, https://www.ebi.ac.uk/pride/archive/projects/PXD033859. Deposited 12 May 2022.